

## Surface Oxide-Support Interaction (SOSI) for Surface Redox Sites

Recent studies of supported vanadium oxide catalysts have revealed that the vanadium oxide component is present as a two-dimensional metal oxide overlayer on oxide supports (i.e.,  $\text{Al}_2\text{O}_3$ ,  $\text{TiO}_2$ ) (1-9). These surface vanadium oxide species are generally more selective and active than bulk, crystalline  $\text{V}_2\text{O}_5$  for the partial oxidation of hydrocarbons (3, 5, 10, 11). The molecular structures of these surface vanadium oxide species have recently been characterized under *in situ* conditions with Raman spectroscopy (4, 12-15), infrared spectroscopy (13), solid-state  $^{51}\text{V}$  NMR spectroscopy (9), and X-ray absorption near edge structure (XANES) spectroscopy (16). The characterization results uniformly agree that under *in situ* conditions the surface vanadium oxide species appears to be four coordinated. In addition, the Raman and infrared vibrational spectroscopy measurements reveal that two different surface vanadium oxide species can be present on the oxide supports. The *in situ* Raman spectra exhibit a sharp band at  $\sim 1030\text{ cm}^{-1}$  and a broad band at  $\sim 900\text{ cm}^{-1}$ , and the relative intensities of these two Raman bands varies with surface vanadium oxide coverage on the oxide support. At low surface coverages the sharp Raman band at  $\sim 1030\text{ cm}^{-1}$  usually dominates, and the broad Raman band at  $\sim 900\text{ cm}^{-1}$  generally grows in at higher surface coverages (with the exception of the  $\text{V}_2\text{O}_5/\text{SiO}_2$  system which does not possess the  $\sim 900\text{ cm}^{-1}$ ). The surface vanadium oxide responsible for the sharp Raman band at  $\sim 1030\text{ cm}^{-1}$  has been assigned to an isolated vanadate species possessing one terminal  $\text{V}=\text{O}$  bond and three bridging  $\text{V}-\text{O}$ -support bonds (9, 12-15, 17), and the broad

Raman band at  $\sim 900\text{ cm}^{-1}$  has been assigned to polymeric tetrahedral metavanadates (9, 17) which are essentially dioxo species. In the present investigation, the physical and chemical properties of the isolated surface vanadate species, corresponding to the Raman band at  $\sim 1030\text{ cm}^{-1}$ , are examined on different oxide supports in order to determine the extent of surface oxide-support interactions for supported vanadium oxide catalysts.

Vanadium oxide catalysts on various oxide supports ( $\text{SiO}_2$ ,  $\text{TiO}_2$ ,  $\text{Nb}_2\text{O}_5$ ,  $\text{Al}_2\text{O}_3$ , and  $\text{ZrO}_2$ ), containing 1%  $\text{V}_2\text{O}_5$  by weight, were prepared by the incipient-wetness impregnation of the nonaqueous vanadium oxide precursor ( $\text{VO}(\text{OC}_3\text{H}_7)_3$ ). The surface areas of  $\text{SiO}_2$  (Cabot, Cabosil),  $\text{TiO}_2$  (Degussa, P-25),  $\text{ZrO}_2$  (Degussa),  $\text{Al}_2\text{O}_3$  (Harshaw), and  $\text{Nb}_2\text{O}_5$  (Niobium Products Company) were 300, 55, 39, 180, and  $60\text{ m}^2/\text{g}$ , respectively. The oxide supports were impregnated with a  $\text{VO}(\text{OC}_3\text{H}_7)_3$ -methanol solution under an  $\text{N}_2$  atmosphere. This was followed by two steps of drying (room temperature for 16 h, and  $120^\circ\text{C}$  for 16 h) and heating at  $350^\circ\text{C}$  in flowing  $\text{N}_2$  (15). Finally,  $\text{V}_2\text{O}_5/\text{SiO}_2$  and  $\text{V}_2\text{O}_5/\text{Al}_2\text{O}_3$  samples were calcined at  $500^\circ\text{C}$  for 16 h;  $\text{V}_2\text{O}_5/\text{TiO}_2$ ,  $\text{V}_2\text{O}_5/\text{ZrO}_2$ , and  $\text{V}_2\text{O}_5/\text{Nb}_2\text{O}_5$  were calcined at  $450^\circ\text{C}$  for 2 h.

The *in situ* Raman spectrometer consists of an *in situ* cell and a Spex 1877 Triplemate spectrometer with a photodiode array detector (EG&G, Princeton Applied Research) (18), and is very similar to the design earlier reported in the literature (4). Excitation was produced with an argon-ion laser (Spectra-Physics, Model 171) which provided 50-100 mW of laser power, as measured at the sample. Raman spectra were collected at  $80^\circ\text{C}$

TABLE 1

*In Situ* Raman of Surface Vanadium Oxide Species on Different Oxide Supports

Oxide support	<i>In situ</i> Raman band position (cm <sup>-1</sup> )	Average C.N. of oxygen anions in oxide supports (20, 21)
SiO <sub>2</sub>	1038	2
Nb <sub>2</sub> O <sub>5</sub>	1031	~2.8(3)
TiO <sub>2</sub>	1030	3
Al <sub>2</sub> O <sub>3</sub>	1026	4
ZrO <sub>2</sub>	1026	4

after the samples were dehydrated at 400–500°C. The spectral resolution and reproducibility were experimentally determined to be approximately 1 cm<sup>-1</sup>. Partial oxidation of methanol was carried out in a differential reactor operating at atmospheric pressure and a temperature of 230°C. Reaction temperatures of 180, 200, and 230°C were used to determine the activation energy. The feed composition consisted of methanol, oxygen, and helium in the ratio 6/11/83 (mol%), flowing at the rate of 25–100 sccm in order to maintain <10% conversion. Products were analyzed with an on-line gas chromatograph (HP 5890) (15).

The influence of the oxide support upon the surface vanadium oxide Raman band position is shown in Table 1. The surface vanadate Raman band shifts from 1038 to 1026 cm<sup>-1</sup> upon changing the oxide support which corresponds to approximately a 0.01 Å (~0.1 valence units) increase in the V=O bond length (19). Consequently, the surface vanadium oxide species on SiO<sub>2</sub> possesses the shortest V=O bond and the surface vanadium oxide species on Al<sub>2</sub>O<sub>3</sub> and ZrO<sub>2</sub> possess the longest V=O bond. This slight change in the surface vanadium oxide species V=O bond length appears to correlate with the coordination of the oxide anions of the different oxide supports (see Table 1), and suggests that the bridging oxygens, V–O–support bonds, may possess a

different coordination number (C.N.) that depends on the specific oxide support (20). For example, on the SiO<sub>2</sub> support V–O–Si bonds are present, on the TiO<sub>2</sub> support V–O(–Ti)<sub>2</sub> bonds are present, on the Al<sub>2</sub>O<sub>3</sub> support V–O(–Al)<sub>3</sub> bonds are present, and on the ZrO<sub>2</sub> support V–O(–Zr)<sub>3</sub> bonds are present. The oxygen anion in Nb<sub>2</sub>O<sub>5</sub> has several coordinations but the average approaches a C.N. of 3 (21), and the agreement with the V<sub>2</sub>O<sub>5</sub>/TiO<sub>2</sub> Raman results suggests that three coordinated oxygen anions may predominate at the surface of Nb<sub>2</sub>O<sub>5</sub>. This trend appears to be analogous to the infrared shift of the C≡O bond which depends on the coordination site of the carbon atom upon adsorption (atop, bridged, or hollow sites) (22). Thus, the physical characteristics of the surface vanadium oxide species are slightly influenced by the specific oxide support to which it is coordinated.

The reactivity of 1% V<sub>2</sub>O<sub>5</sub> on the different oxide supports was probed with the methanol oxidation reaction. The 1% V<sub>2</sub>O<sub>5</sub> loading was chosen because crystalline V<sub>2</sub>O<sub>5</sub> was not present in any of the supported vanadium oxide catalysts at this loading, and the surface vanadate species responsible for the sharp Raman band at ~1030 cm<sup>-1</sup> was the only (SiO<sub>2</sub> and TiO<sub>2</sub>) or the predominant (Nb<sub>2</sub>O<sub>5</sub>, Al<sub>2</sub>O<sub>3</sub>, and ZrO<sub>2</sub>) surface species present (18). The SiO<sub>2</sub>, TiO<sub>2</sub>, ZrO<sub>2</sub>, and Nb<sub>2</sub>O<sub>5</sub> supports were essentially inactive for methanol oxidation, but the Al<sub>2</sub>O<sub>3</sub> support was very active for the conversion of methanol to dimethyl ether and the reactivity of the V<sub>2</sub>O<sub>5</sub>/Al<sub>2</sub>O<sub>3</sub> catalyst had to be corrected for the alumina support reactivity. The reaction rates were normalized per surface vanadium oxide species since the Raman measurements demonstrated that the vanadium oxide was 100% dispersed on the support surface. The turnover rate for methanol oxidation over the different supported vanadium oxide catalysts were found to vary by three orders of magnitude as shown in Table 2. Formaldehyde was almost exclusively formed on all the supported vanadium oxide catalysts with the exception of V<sub>2</sub>O<sub>5</sub>/Al<sub>2</sub>O<sub>3</sub>

TABLE 2  
Reactivity of Surface Vanadium Oxide Species on  
Different Oxide Supports

Catalysts	Turnover rate Rate (sec <sup>-1</sup> )	$T_{\max}$ (K) <sup>a</sup>	$T_{\text{start}}$ (K) <sup>b</sup>
1% V <sub>2</sub> O <sub>5</sub> /SiO <sub>2</sub>	$2.0 \times 10^{-3}$	790	>650
Bulk V <sub>2</sub> O <sub>5</sub>	$2.0 \times 10^{-2}$	790	750
1% V <sub>2</sub> O <sub>5</sub> /Al <sub>2</sub> O <sub>3</sub>	$2.6 \times 10^{-2c}$	743	650
1% V <sub>2</sub> O <sub>5</sub> /Nb <sub>2</sub> O <sub>5</sub>	$7.0 \times 10^{-1}$	— <sup>d</sup>	— <sup>d</sup>
1% V <sub>2</sub> O <sub>5</sub> /TiO <sub>2</sub>	$1.8 \times 10^0$	715	600
1% V <sub>2</sub> O <sub>5</sub> /ZrO <sub>2</sub>	$2.3 \times 10^0$	723	520

<sup>a</sup> Maximum temperature of reduction, from Ref. (23).

<sup>b</sup> Onset temperature of reduction, from Ref. (24).

<sup>c</sup> Corrected for significant reactivity of oxide support. The uncorrected reactivity of the 1% V<sub>2</sub>O<sub>5</sub>/Al<sub>2</sub>O<sub>3</sub> catalysts, predominantly yields dimethyl ether and traces of formaldehyde. The turnover rate of 1% V<sub>2</sub>O<sub>5</sub>/Al<sub>2</sub>O<sub>3</sub> was calculated from the amount of formaldehyde formed.

<sup>d</sup> Not determined.

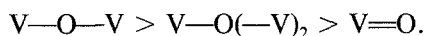
which formed dimethyl ether because of the highly reactive acid sites present on the Al<sub>2</sub>O<sub>3</sub> support. These reactivity studies demonstrate that essentially the same surface vanadium oxide species exhibits vastly different reactivities which markedly depend on the specific oxide support (surface oxide-support interaction (SOSI)).

Comparison of the *in situ* Raman and reactivity data reveals that the dramatic promotional effect of the oxide supports upon the surface vanadium oxide species is not related to the slight perturbations upon the V=O and V-O-support bonds. The two extreme surface vanadium oxide species occur on the SiO<sub>2</sub> (~1038 cm<sup>-1</sup>) and the Al<sub>2</sub>O<sub>3</sub> (~1026 cm<sup>-1</sup>) oxide supports and both of these systems represent the least active supported vanadium oxide catalysts. Furthermore, the surface vanadium oxide species on Al<sub>2</sub>O<sub>3</sub> and ZrO<sub>2</sub> possess Raman bands at ~1026 cm<sup>-1</sup> and exhibit vastly different reactivities. Consequently, the slight perturbation on the surface vanadium oxide molecular structures by the oxide supports do not appear to influence their reactivity.

The promotional effect of the oxide supports upon the reactivity of the surface vanadium oxide species appears to be related to the reducibility of the supported vanadium oxide catalysts. The chosen experimental conditions of excess oxygen partial pressure (zero order with respect to oxygen partial pressure) correspond to the reduction step as the slow and rate-determining step in the redox cycle. Comparison of the turnover rates with the corresponding temperatures for the onset of reduction during temperature-programmed reduction experiments (see Table 2) reveals a similar trend, and further confirms that the reduction step is the slow step during methanol oxidation over the supported vanadium oxide catalysts. Furthermore, the reducibilities of the supported vanadium oxide catalysts appear to follow the intrinsic reducibilities of the pure oxide supports (25a). Similar studies with supported molybdenum oxide catalysts result in a corresponding turnover frequency trend with reactivities that are approximately an order of magnitude lower than those for supported vanadium oxide catalysts, and suggests that the overall reduction characteristics of supported metal oxide catalysts are also dependent on the specific surface metal oxide species (26). The strong influence of the oxide support on the reactivity of surface metal oxide species at low coverages (supported vanadium oxide and supported molybdenum oxide) suggests that the bridging M-O-support bonds (M = V, Mo), rather than the terminal M=O bonds (M = V, Mo), are associated with the active sites during methanol oxidation.

The conclusion that the bridging M-O-support bonds, rather than the terminal M=O bonds, are associated with the active sites is consistent with several recent experimental findings and theoretical calculations of metal oxides (27, 28). Reactivity studies of the behavior of oriented MoO<sub>3</sub> single crystals demonstrated that on the (010) plane, which contains primarily Mo=O bonds, only physical adsorption of methanol takes place without any chemical transfor-

mations, but on surfaces perpendicular to this plane, which contain Mo–O–Mo and Mo–OH bonds, methoxy groups are formed at room temperature and convert to formaldehyde at higher temperatures (27). Quantum chemical calculations for adsorption of hydrogen molecules on the different sites present in crystalline  $V_2O_5$  have revealed the following reactivity pattern (28)



Thus, the terminal  $M=O$  bonds in metal oxides appear to be more stable than the bridging  $M-O-M$  bonds in metal oxides, and, consequently, the reactivity of metal oxide catalysts is dominated by the bridging functionalities.

The  $V-O$ -support bond reduction characteristics and the reactivity toward methanol oxidation, which is also a reduction process since the redox step is the slow reaction step, follow the same trend (see Table 2), and are directly influenced by the *surface* reduction characteristics of the oxide support. For example, both the bulk and surface sites readily reduce for  $TiO_2$  and  $Nb_2O_5$ , but not for  $Al_2O_3$  and  $SiO_2$  (25a). Zirconia, on the other hand, is readily reduced at the surface but not in the bulk (25b). Thus, methods that measure the bulk reducibilities of metal oxides, such as ordering the oxides with respect to their reducibility in terms of the thermodynamic equilibrium ( $p_{H_2O}/p_{H_2}$ ) between the starting saturated oxide and a lower valence oxide (25a), will not be able to predict the reactivity patterns observed for the supported vanadium oxide catalysts since it is critical to have information on surface reduction characteristics. For example, the zirconia system is predicted to be essentially irreducible from thermodynamic equilibrium measurements (25a), a reflection of its bulk properties, but readily reduces at its surface as shown by XPS measurements (25b). In the absence of quantitative information in the literature about the *surface* reduction characteristics of metal oxides, the reduction behavior of supported vanadium oxide

catalysts from temperature-programmed reduction experiments appear to be the most reliable measure of catalytic reactivity since it directly probes the reactivity of the critical surface  $V-O$ -support bond, which is more relevant than the reducibility of the pure oxide support surface.

The dramatic influence of the oxide support upon the supported vanadium oxide catalysts during methanol oxidation is due to the influence of the oxide support on the reduction properties of the  $V-O$ -support bond. The oxide support may be influencing the number of active surface sites, if all surface vanadia sites are not simultaneously participating in the catalytic cycle, or the activity per surface site (i.e., the oxygen vacancies created during the redox cycle may facilitate the migration of lattice oxygen from the support onto the surface).

Kinetic studies have revealed that essentially the same activation energy,  $18.3 \pm 0.9$  kcal/mol, occurs over supported vanadium oxide catalysts during methanol oxidation, with the exception of 1%  $V_2O_5/SiO_2$ . For 1%  $V_2O_5/SiO_2$ , the activation energy has not been determined since the reaction rate is below detection limit at the lower temperatures (180 and 200°C). The activation energy of the supported vanadium oxide catalysts is similar to the value found for breaking the C–H bond of  $CH_3O_{ads}$  surface intermediates during transformation to formaldehyde (29). The similar activation energy measured for methanol oxidation over the surface vanadium oxide on the different oxide supports suggests that the same rate-determining step is occurring on all the supported vanadium oxide catalysts, and that the difference in activity is due to the preexponential factor which may be related to the number of active sites or activity per site. Additional transient experiments are necessary to confirm this conclusion.

The influence of the oxide support on the catalytic properties of supported vanadium oxide catalysts has been known over the past decade, but the origin of this phenomenon was not identified. Hauffe and Raveling

examined the oxidation of *o*-xylene over a series of supported vanadium oxide catalysts and the best catalytic performance was obtained with a  $\text{TiO}_2$  support, followed by  $\text{SnO}_2$  and  $\text{ZrO}_2$  (30). These authors explained their results on the basis of the influence of the oxide substrate on the defect structure of the supported vanadium oxide phase. Murakami *et al.* investigated the reaction rates for several different reactions over a series of supported vanadium oxide catalysts and found that the reaction rates depend both on the nature of the oxide support and the kind of reactant molecule (31). Roozeboom *et al.* studied the methanol oxidation reaction and carbon monoxide oxidation reaction over supported vanadium oxide catalysts (24, 32). The reaction rates were found to vary with the nature of the oxide support ( $\text{Al}_2\text{O}_3$ ,  $\text{CeO}_2$ ,  $\text{TiO}_2$ , and  $\text{ZrO}_2$ ) and a direct correlation between the catalyst activity and its reducibility was found in these studies. Roozeboom *et al.* unsuccessfully attempted to correlate the catalytic behavior of the supported vanadium oxide catalysts with the bulk properties of the oxide support, i.e., the ratio of the carrier cation to the sum of the radii of carrier cation and oxide anion, rather than the *surface* properties of the supported vanadium oxide phase or of the oxide support. The present *in situ* Raman structural characterization and reactivity studies reveal that the catalytic behavior of supported vanadium oxide catalysts are directly related to the reduction characteristics of the *surface* V–O–support bonds.

In summary, *in situ* Raman studies reveal that the same surface vanadium oxide species, isolated vanadate species possessing one terminal V=O bond and three bridging V–O–support bonds, preferentially exists on the  $\text{SiO}_2$ ,  $\text{Nb}_2\text{O}_5$ ,  $\text{TiO}_2$ ,  $\text{Al}_2\text{O}_3$ , and  $\text{ZrO}_2$  supports at low vanadium oxide surface coverages. The different oxide supports only slightly perturb the vanadium–oxygen bond lengths of the surface vanadium oxide species. The reactivity studies reveal that essentially the same surface vanadium oxide

species exhibits vastly different reactivity during partial oxidation of methanol which markedly depend on the specific oxide support. The dramatic promotional effect of the oxide support upon the reactivity of the surface vanadium oxide species, surface oxide–support interaction, is related to the reducibility of the specific oxide support surface. This suggests that the bridging V–O–support bonds, rather than the terminal V=O bonds, are associated with the active sites during oxidation reactions. The parallel influence of the oxide support upon the supported metal oxide systems (surface oxide–support interaction) and the supported metal systems (strong metal–support interaction (SMSI)) are very striking and appear to follow a similar pattern (33). Thus, oxide supports known to exhibit the SMSI phenomenon are expected to enhance the oxidation rates of supported metal oxide catalysts.

#### ACKNOWLEDGMENTS

Financial Support by NSF Grant No. CBT-88107141 and CTS-9006258 is gratefully acknowledged.

#### REFERENCES

1. Roozeboom, F., Mittelmeijer-Hazeleger, M. C., Moulijn, J. A., Medema, J., de Beer, V. H. J., and Gellings, P. J., *J. Phys. Chem.* **84**, 2783 (1980).
2. Kozłowski, R., Pettifer, R. F., and Thomas, J. M., *J. Phys. Chem.* **87**, 5176 (1983).
3. van Hengstum, A. J., van Ommen, J. G., Bosch, H., and Gellings, P. J., *Appl. Catal.* **5**, 207 (1983).
4. Chan, S. S., Wachs, I. E., Murrell, L. L., Wang, L., and Hall, W. K., *J. Phys. Chem.* **88**, 5831 (1984).
5. Wachs, I. E., Saleh, R. Y., Chan, S. S., and Chersich, C. C., *Appl. Catal.* **15**, 339 (1985).
6. Haber, J., Kozłowska, A., and Kozłowski, R., *J. Catal.* **102**, 52 (1986).
7. Wachs, I. E., Hardcastle, F. D., Chan, S. S., *Mater. Res. Soc. Symp. Proc.* **111**, 353 (1988).
8. Hardcastle, F. D., and I. E. Wachs, in "Proceedings, 9th International Congress on Catalysis, Calgary, 1988" (M. J. Phillips and M. Ternan, Eds.), Vol. 3, p. 1449. Chem. Institute of Canada, Ottawa, 1988.
9. Eckert, H., and Wachs, I. E., *J. Phys. Chem.* **93**, 6796 (1989).
10. Bond, G. C., and Bruckman, K., *Faraday Discuss. Chem. Soc.* **72**, 235 (1981).

11. Gasior, M., Gasior, I., and Grzybowska, B., *Appl. Catal.* **10**, 87 (1984).
12. Oyama, S. T., Went, G., Lewis, K. B., Bell, A. T., Somarjai, G., *J. Phys. Chem.* **93**, 6786 (1989); Went, G. T., Oyama, S. T., and Bell, A. T., *J. Phys. Chem.* **94**, 4240 (1990).
13. Cristianini, C., Forzatti, P., Busca, G., *J. Catal.* **116**, 586 (1989).
14. Le Costumer, L. R., Taouk, B., Le Meur, M., Payen, E., Guelton, M., and Grimblot, J., *J. Phys. Chem.* **92**, 1230 (1988).
15. Deo, G., Eckert, H., and Wachs, I. E., *Prepr. Am. Chem. Soc. Div. Petrol. Chem.* **35**(1), 16 (1990).
16. Yoshida, S., Tanaka, T., Nishimura, Y., Mizutani, H., and Funabiki, T., in "Proceedings, 9th International Congress on Catalysis, Calgary, 1988" (M. J. Phillips and M. Ternan, Eds.), Vol 3, p. 1473. Chem. Institute of Canada, Ottawa, 1988.
17. Wachs, I. E., *J. Catal.* **124**, 570 (1990).
18. Deo, G., Vuorman, M., Wachs, I. E., in press.
19. Hardcastle, F. D., and Wachs, I. E., *J. Phys. Chem.*, in press.
20. Boehm, H.-P., and Knözinger, H., in "Catalysis: Science and Technology" (J. R. Anderson and M. Boudart, Eds.), Vol 4, p. 39. Springer-Verlag, Berlin/Heidelberg, 1983.
21. Ikeya, T., and Senna, M., *J. Non-Cryst. Solids* **105**, 243 (1988).
22. Eischens, R. P., and Pliskin, W. A., in "Advances in Catalysis" (D. D. Eley, W. G. Frankenburg, and V. I. Komarewsky, Eds.), Vol. 10, p. 1. Academic Press, New York, 1958; Hulse, J. E., and Moskovits, M., *Surf. Sci.* **59**, 205 (1976).
23. Bond, G. C., Flamerz, S., and Shukri, R., *Faraday Discuss. Chem. Soc.* **87**, 65 (1989).
24. Roozeboom, F., Jos van Dillen, A., Geus, J. W., and Gellings, P. J., *Ind. Eng. Chem. Prod. Res. Dev.* **20**, 304 (1981).
25. (a) Tauster, S. J., Fung, S. C., Baker, R. T. K., and Horsley, J. A., *Science* **221**, 1121 (1981); (b) Tauster, S. J., *Acc. Chem. Res.* **20**, 389 (1987).
26. Deo, G., D. S. Kim, K. Segawa, and Wachs, I. E., in press.
27. Ohuchi, F., Fирment, L. E., Chowdry, U., Ferretti, A., *J. Vac. Sci. Technol., A* **2**, 1022 (1984).
28. Haber, J., private communication.
29. Farneth, W. E., Ohuchi, F., Staley, R. H., Chowdry, U. and Sleight, A. W., *J. Phys. Chem.* **89**, 2493 (1985).
30. Hauffe, K., and Raveling, H., *Ber. Bunsenges. Phys. Chem.* **84**, 912 (1980).
31. Murakami, Y., Inamoto, M., Miyamoto, A., and Mori, K., in "Proceedings, 7th International Congress on Catalysis, Tokyo, 1980" (T. Seiyama and K. Tanabe, Eds.), p. 1344. Elsevier, Amsterdam, 1981.
32. Roozeboom, F., Cordingley, P. D., and Gellings, P. J., *J. Catal.* **68**, 464 (1981).
33. Hegedus, L. L., Aris, R., Bell, A. T., Boudart, M., Chen, N. Y., Gates, B. C., Haag, W. O., Wei, J., "Catalysis Design Progress and Perspectives," Chap. 4. Wiley, New York, 1987.

GOUTAM DEO  
ISRAEL E. WACHS

*Zettlemoyer Center for Surface Studies  
Department of Chemical Engineering  
Lehigh University  
Bethlehem, Pennsylvania 18015*

*Received June 12, 1990; revised December 12, 1990*